

# A Theoretical Study of Phase Behaviors for Diblock Copolymers in Selective Solvents

Tongchuan Suo,<sup>†</sup> Dadong Yan,<sup>\*,†</sup> Shuang Yang,<sup>†</sup> and An-Chang Shi<sup>‡</sup>

<sup>†</sup>Beijing National Laboratory for Molecular Sciences (BNLMS), Institute of Chemistry, Chinese Academy of Sciences, Beijing, 100190, China, and <sup>‡</sup>Department of Physics and Astronomy, McMaster University, Hamilton, Ontario L8S 4M1, Canada

Received April 30, 2009; Revised Manuscript Received July 13, 2009

**ABSTRACT:** A self-consistent mean-field theory (SCMFT) study on the phase behaviors of AB-diblock copolymer solutions is presented. All of the possible thermodynamically stable ordered structures verified by experiments are considered and the phase diagrams are generated. This work mainly focuses on the cases of selective solvents. The results show that a series of phase transitions occurs upon dilution. In particular, large windows of lamellae + cylinder coexistence are located for the cases of highly asymmetric diblock copolymers in strongly selective solvents, which is in agreement with previous experimental observations. The transitions between the “inverted” fcc structure and the “inverted” bcc structure are also observed. The calculation indicates that the copolymer–solvent interaction plays important roles in these transitions.

## Introduction

As a good system to study the phenomenon of self-assembling, diblock copolymer solution has attracted considerable attention. Much work has been done in this field both experimentally and theoretically. Generally speaking, all solvents can be divided into two kinds: one is neutral solvent, which has the same interaction with each block species; the other is selective solvent, which interacts with the two blocks differently. With the presence of the solvent, diblock copolymer solution always has more interesting phase behaviors than melt does.

When the solvent is neutral, it will equally swell each block of the diblock copolymer, which just leads to a dilution effect. It has been shown by previous experimental and theoretical work<sup>1–7</sup> that the phase behavior in this case is very similar to diblock copolymer melt. Namely, the microstructure of the system is largely determined by the composition of the copolymer while the dilution effect caused by solvent mainly changes the degree of segregation.

If a selective solvent is added, the two kinds of blocks are swollen unequally. The solvent now prefers to aggregate more into the domain of one species than the other, which consequently leads to a series of lyotropic ordered structure transitions. There is a great deal of experimental and theoretical studies on this case. From the experimental standpoint, Shibayama and co-workers first gave a study on the microstructure of a diblock copolymer (polystyrene-*b*-polybutadiene) in a selective solvent (*n*-tetradecane).<sup>8,9</sup> Afterward, the phase behaviors of diblock copolymers in selective solvents have been revealed gradually. On one hand, aqueous diblock copolymer solution system has received much attention. For example, Hajduk and co-workers investigated aqueous solutions of poly(ethylene oxide)-*b*-polyethylethylene and constructed the phase diagrams.<sup>10</sup> However, because of the existence of hydrogen bonding and the lower-critical-solution-temperature (LCST) character, the phase behaviors of an aqueous system are often less common and have little theoretical correspondence. On the other hand, there is also much work on

the self-assembly of a diblock copolymer in the presence of an organic selective solvent, particularly in the cases of styrene-isoprene diblock copolymers. Among the numerous literatures on this subject, a series of studies done by Lodge and co-workers gave a comprehensive description of the issue.<sup>11–13</sup> Within their work, not only have the complete phase diagrams been constructed, but also the general principles have been discussed. Accompanying with these experimental progresses, theoretical developments also come. Banaszak and Whitmore first used the self-consistent mean-field theory (SCMFT) to investigate the lamellar structure of diblock copolymer/selective solvent blends.<sup>14</sup> Although they only dealt with weakly selective solvents, some universal properties, such as the nonuniform distribution of the solvent, are revealed. Huang and co-workers extended the previous SCMFT calculations to consider ordered structures other than lamellar and gave some sectional planes of the diblock copolymer solution phase hypercube (i.e., phase diagrams).<sup>15,16</sup> However, their calculations are incomplete because of the high dimension of the parameter space of the theoretical model. Also the neglect of the gyroid structure makes it impossible for them to verify the lamellae + cylinder coexistence, which is observed by experiments.<sup>10,12,13</sup> Most recently, Woloszczuk et al. constructed a phase diagram of a diblock copolymer solution using a lattice Monte Carlo method,<sup>17</sup> in which only the symmetric diblock copolymer was considered.

It is well-known that SCMFT has been applied to study a great deal of problems in polymeric systems. Compared with other theoretical methods, such as Monte Carlo methods<sup>17</sup> and field simulations,<sup>18</sup> SCMFT is much easier to perform and so is more appropriate to study some complex systems, such as multiblock copolymers and copolymer solutions. Hence we apply SCMFT in this paper to investigate the phase behavior of diblock copolymers in the presence of a selective solvent. All of the possible thermodynamically stable ordered structures verified by experiments are considered and the phase diagrams are generated. Large windows of lamellae + cylinder coexistence are located in addition to the traditional structures. The physics hidden in these results are also discussed.

\*Corresponding author. E-mail: yandd@iccas.ac.cn.

## Theoretical Framework

**Self-Consistent Mean-Field Theory.** The system is composed of  $n_c$  AB diblock copolymer (C) chains and  $n_s$  solvent (S) molecules in a volume  $V$ . Each AB chain of degree of copolymerization  $N$  contains  $fN$  A monomers and  $(1-f)N$  B monomers. For simplicity, we assume that all monomers have the same volume  $\rho_0^{-1}$  as the solvent and the same Kuhn length  $b$ . Since  $n_c$  and  $n_s$  are constant, the canonical ensemble is used here. Following a standard field theory procedure,<sup>19,20</sup> the partition functional can be written as

$$Z = \int \mathcal{D}\{\phi\} \mathcal{D}\{\omega\} \mathcal{D}\{\eta\} e^{-\mathcal{F}[\{\phi\}, \{\omega\}, \{\eta\}]} \quad (1)$$

where the “Hamiltonian” of the system,  $\mathcal{F}[\{\phi\}, \{\omega\}, \{\eta\}]$ , is given by

$$\begin{aligned} \mathcal{F}[\{\phi\}, \{\omega\}, \{\eta\}] = & \frac{1}{2} \sum_{\alpha \neq \beta} \rho_0 \chi_{\alpha\beta} \int d\mathbf{r} \phi_\alpha(\mathbf{r}) \phi_\beta(\mathbf{r}) \\ & - \sum_\alpha \frac{\rho_0}{N} \int d\mathbf{r} \omega_\alpha(\mathbf{r}) \phi_\alpha(\mathbf{r}) + \frac{\rho_0}{N} \int d\mathbf{r} \eta(\mathbf{r}) \left( \sum_\alpha \phi_\alpha(\mathbf{r}) - 1 \right) \\ & - \rho_0 V \sum_p \frac{\bar{\phi}_p}{N_p} \ln \frac{z_{0p} e N_p Q_p}{\rho_0 \bar{\phi}_p} \end{aligned} \quad (2)$$

In eq 2,  $\alpha, \beta = A, B, S$ ;  $p = C, S$ ;  $\chi_{\alpha\beta}$  is the Flory–Huggins parameter, which quantifies the local interaction between each pair of units  $\alpha$  and  $\beta$ ;  $\phi_\alpha(\mathbf{r})$  is the volume fraction of species  $\alpha$  at point  $\mathbf{r}$ ;  $\omega_\alpha(\mathbf{r})$  is the auxiliary field conjugated to  $\phi_\alpha(\mathbf{r})$ ;  $\eta(\mathbf{r})$  is the auxiliary field coupled to the incompressible condition;  $\bar{\phi}_p$  is the average volume fraction of component  $p$ ;  $N_p = N$  and 1 for  $p = C$  and  $S$ , respectively;  $z_{0p}$  is the partition function of component  $p$  due to the kinetic energy, which can be regarded as a constant;  $Q_p$  is the partition function of a single molecule of component  $p$ .

To evaluate the partition functional exactly is in general impossible. Fortunately, the mean field approximation is available here, which amounts to evaluating the functional integral using a saddle-point technique.<sup>19,20</sup> By this approximation, the problem of dealing with the functional integral is converted to solving a set of mean-field equations

$$\phi_A(\mathbf{r}) = \frac{\bar{\phi}_C}{Q_C} \int_0^f dt q_A(\mathbf{r}, t) q_A^+(\mathbf{r}, t) \quad (3)$$

$$\phi_B(\mathbf{r}) = \frac{\bar{\phi}_C}{Q_C} \int_0^{1-f} dt q_B(\mathbf{r}, t) q_B^+(\mathbf{r}, t) \quad (4)$$

$$\phi_S(\mathbf{r}) = \frac{\bar{\phi}_S}{Q_S} q_S \left( \mathbf{r}, \frac{1}{N} \right) \quad (5)$$

$$\omega_\alpha(\mathbf{r}) = N \sum_{\beta \neq \alpha} \chi_{\alpha\beta} \phi_\beta + \eta(\mathbf{r}) \quad (6)$$

$$\sum_\alpha \phi_\alpha(\mathbf{r}) = 1 \quad (7)$$

Here,  $t$  is the coordinate along a copolymer chain, which has been scaled by  $N$ . Each of the end-integrated propagators,

$q_\alpha(\mathbf{r}, f)$ , satisfies the modified diffusion equation

$$\frac{\partial q_\alpha(\mathbf{r}, t)}{\partial t} = \frac{Nb_\alpha^2}{6} \nabla^2 q_\alpha(\mathbf{r}, t) - \omega_\alpha(\mathbf{r}) q_\alpha(\mathbf{r}, t) \quad (8)$$

with the initial condition,  $q_\alpha(\mathbf{r}, 0) = 1$ . In the present calculations, all lengths are scaled by  $b$ . Thus in eq 8,  $b_\alpha = 1$  for  $\alpha = A, B$ , and  $b_\alpha = 0$  for  $\alpha = S$ .  $q_A^+(\mathbf{r}, t)$  and  $q_B^+(\mathbf{r}, t)$  also satisfy eq 8 but with different initial conditions,  $q_A^+(\mathbf{r}, 0) = q_B(\mathbf{r}, 1-f)$  and  $q_B^+(\mathbf{r}, 0) = q_A(\mathbf{r}, f)$ .

Since we are dealing with the symmetric structures, the reciprocal-space method is convenient. Every function of position is expanded by a set of orthonormal basis functions  $\{f_i(\mathbf{r})\}$ , which possesses the symmetry of the structure being considered, e.g.

$$\phi_\alpha(\mathbf{r}) = \sum_{i=1}^{\infty} \phi_i^\alpha f_i(\mathbf{r})$$

The expansions of other functions are similar, and the unnormalized basis functions can be found in ref 21. Sufficient number of basis functions should be used to have enough numerical precision in any case. The number required is different for different structures and parameter values. Within the parameter ranges used here, eighty basis functions are enough for lamellae and hexagonally packed cylinders. However, for those more complex structures, e.g. body-centered cubic and face-centered cubic spheres, about 200 basis functions are needed when  $\bar{\phi}_C \rightarrow 1$  and more than 400 basis functions are required for low  $\bar{\phi}_C$  but high  $\chi_{BS}$ . Gyroid is the most complicated structure considered here, for which the number required is always 50 more than the requirement for cubic spheres in the same parameter values.

By reciprocal-space method, we only need to solve the expansion coefficients. The equations of these coefficients can be derived from the SCMFT equations

$$\phi_i^A = \frac{\bar{\phi}_C}{Q_C} \int_0^f dt \sum_{m,l} q_m^A(t) q_l^{A+}(f-t) \Gamma_{iml} \quad (3')$$

$$\phi_i^B = \frac{\bar{\phi}_C}{Q_C} \int_0^{1-f} dt \sum_{m,l} q_m^B(t) q_l^{B+}(1-f-t) \Gamma_{iml} \quad (4')$$

$$\phi_i^S = \frac{\bar{\phi}_S}{Q_S} q_i^S \left( \frac{1}{N} \right) \quad (5')$$

$$\omega_i^\alpha = N \sum_{\beta \neq \alpha} \chi_{\alpha\beta} \phi_i^\beta + \eta_i \quad (6')$$

$$\sum_\alpha \phi_i^\alpha = \delta_{i,1} \quad (7')$$

where  $\Gamma_{iml} = V^{-1} \int d\mathbf{r} f_i(\mathbf{r}) f_m(\mathbf{r}) f_l(\mathbf{r})$ ;  $\delta_{i,1}$  is the Kronecker delta function.  $Q_C$  and  $Q_S$  can be expressed as

$$Q_C = q_1^{A+}(f) \quad \text{and} \quad Q_S = q_1^S \left( \frac{1}{N} \right)$$

Note that each of the basis functions is an eigenfunction of Laplacian operator with eigenvalue  $\lambda_i$ . Then the modified

diffusion equation becomes

$$\frac{\partial q_i^\alpha}{\partial t} = - \sum_m H_{im} q_m^\alpha \quad (8')$$

where

$$H_{im} = \frac{Nb_\alpha^2}{6} \lambda_i \delta_{i,m} + \sum_l \omega_l^\alpha \Gamma_{iml}$$

The initial conditions of  $q_i^\alpha(t)$  and  $q_i^{\alpha+}(t)$  are:  $q_i^\alpha(0) = \delta_{i,1}$ ;  $q_i^{\alpha+}(0) = q_i^\beta(f_\beta)$ , where  $\beta = B$  when  $\alpha = A$  and vice versa.

After solving these equations by certain iteration technique, the free energy (in the unit of  $k_B T$ ) per chain of the system can be obtained

$$F = \frac{N}{\rho_0 V} \mathcal{F} = \frac{N}{2} \sum_{\alpha \neq \beta} \sum_i \chi_{\alpha\beta} \phi_i^\alpha \phi_i^\beta - \sum_\alpha \sum_i \omega_i^\alpha \phi_i^\alpha - \bar{\phi}_C \ln Q_C - N \bar{\phi}_S \ln Q_S + \bar{\phi}_C \ln \bar{\phi}_C + N \bar{\phi}_S \ln \bar{\phi}_S + \text{const} \quad (9)$$

In this work, five ordered periodic structures are considered, i.e. lamellae (L), hexagonally packed cylinders (H), gyroid (G), body-centered cubic spheres ( $S^{\text{bcc}}$ ) and face-centered cubic spheres ( $S^{\text{fcc}}$ ). Phase lines are determined not only by comparing the free energies of different structures but also by considering the common tangent rule.

**More about the Model.** The parameter space of a polymeric system is always of high dimension. Vavasour and Whitmore identified that at least eight parameters are needed to predict the equilibrium morphology of a diblock copolymer/homopolymer blend,<sup>22</sup> which is similar for the system considered here. Since we are now just interested in diblock copolymers of symmetric conformation, i.e.  $b_A = b_B = b$ , only six parameters need to be considered in this work, i.e., the average volume fraction of the diblock copolymer,  $\bar{\phi}_C$ , the copolymer composition,  $f$ , the degree of copolymerization,  $N$ , and three Flory–Huggins parameters,  $\chi_{\alpha\beta}$ .

However, some of these parameters are less significant than others for studying the physics of self-assembly in diblock copolymer solutions. First, it has been indicated by previous work that the variation of  $N$  always causes few effects on the order–order transitions (OOTs) for copolymer melts. This can be easily understood by using the phase diagram of the melt case,<sup>23</sup> in which the phase lines quickly become vertical to the  $f$ -axis when the system is beyond the weak segregation regime. Although the case is more complex with the presence of a selective solvent, it is confirmed by experiments<sup>7,12,13</sup> and the present calculation (in next section) that the variation of  $N$  brings considerable effects on the order–disorder transition (ODT) rather than OOT. Second, it is always unnecessary to change all the three  $\chi_{\alpha\beta}$  to explore the phase behaviors of the system. This is because the selectivity of the solvent is much more important for determining the symmetric phases than the absolute value of each  $\chi_{\alpha\beta}$ . It is not easy to define selectivity very strictly, but to some extent one can estimate it by the difference between  $\chi_{AS}$  and  $\chi_{BS}$ , i.e.  $(\chi_{BS} - \chi_{AS})/\chi_{AB}$ . In this study, we fix the values of  $\chi_{AB}$  and  $\chi_{AS}$  and make  $\chi_{BS}$  always greater than  $\chi_{AS}$  in order to present an elementary investigation of the effects of solvent selectivity. Thus increasing  $\chi_{BS}$  corresponds to increasing the selectivity of the solvent hereafter. From the experimental standpoint, the selectivity of a specific solvent always changes with varying temperature. Therefore changing  $\chi_{BS}$  in this work

also qualitatively corresponds to changing temperature in practice. In brief, we mainly investigate the effects of three parameters, i.e.  $\bar{\phi}_C$ ,  $f$ , and  $\chi_{BS}$ , in this work. The subspace of  $(\bar{\phi}_C, f, \chi_{BS})$  can be regarded as an appropriate analogy of the phase cube  $(\bar{\phi}_C, f, T)$  in practice.

There is another useful concept called “degree of segregation”, which is related to the sharpness of the interface between different domains and the interfacial area per chain in a symmetric phase. This concept can be quantified by  $\chi_{AB} N$  for an AB-diblock copolymer melt or by  $\bar{\phi}_C \chi_{AB} N$  for the case of an AB-diblock copolymer in a neutral solvent. No simple combination of parameters can be abstracted to describe the degree of segregation for the selective solvent case, but the meaning is the same. Namely, a higher degree of segregation means a sharper interface between different domains and smaller interfacial area per chain in a symmetric phase and vice versa.

## Results

The phase diagrams  $(\bar{\phi}_C, \chi_{BS})$  of different compositions and different degrees of copolymerization are presented in Figure 1. Some general features can be found from the figure. When the copolymer concentration is high, i.e.  $\bar{\phi}_C \rightarrow 1$ , the structure of the system returns to the one of the melt case. Upon dilution, a series of lyotropic structure transitions occur. If the solvent selectivity is high, e.g.  $\chi_{BS} \geq 0.7$  in Figure 1, the two blocks of the copolymer will be swollen much more unequally. In particular, when the copolymer is asymmetric and the solvent prefers the shorter block, the so-called “inverted” phases, in which the swollen shorter block plus solvent forms the major domain, are formed with the decreasing of  $\bar{\phi}_C$ . On the other hand, when the solvent becomes weakly selective with decreasing  $\chi_{BS}$ , the possible phase transitions become fewer, and the system finally coincides with the case of neutral solvent as  $\chi_{BS} = \chi_{AS}$ .

Parts a and b of Figure 1 are the phase diagrams for two symmetric copolymers with different degrees of copolymerization in solvents of varying selectivity. Both figures display a sequence of  $L \rightarrow G_B \rightarrow H_B \rightarrow S_B^{\text{bcc}}$  via dilution in the strongly selective solvent region, while only the transition of  $L \rightarrow \text{Dis}$  occurs as the solvent is weakly selective. There is a small existence window of  $S_B^{\text{fcc}}$  in Figure 1b. We infer that  $S_B^{\text{fcc}}$  also emerges in Figure 1a for larger  $\chi_{BS}$ , although the calculation is too hard to perform there because of the large amount requirement of basis functions. Each OOT line in these two figures tilts to the right for relatively large  $\chi_{BS}$  but to the left when  $\chi_{BS}$  is medium-sized. Thus there is a “reentrant” OOT via varying  $\chi_{BS}$ . After all, it can be seen that these two figures have very similar topologies. Only the ODT lines have considerable difference, which is also quantitative. This is a direct reflection of the fact that the variation of  $N$  has few effect on OOTs and hence hardly affects the topology of each phase diagram. Hence, we just give the diagrams of  $N = 150$  hereafter.

Figure 1c is for an asymmetric diblock copolymer, i.e.,  $f = 0.3$ . In this case, the phase behavior becomes more complex. All possible structures are observed except  $S_A^{\text{fcc}}$ . Several “reentrant” OOTs occur for the “inverted” structures while the phase line that separates two normal structures just tilts to the right. Moreover, an interesting phenomenon can be observed, which is the emergence of the large existence window of  $S_B^{\text{fcc}}$ . When the composition of the diblock copolymer becomes more asymmetrical, the solution goes into disorder at high copolymer concentration. However, if the solvent has enough selectivity, micelle can form via dilution and then ordered structures also emerge, as indicated by Figure 1d. Particularly, it can be seen from Figure 1d that the existence window of  $G_B$  is substituted by an  $L + H_B$  coexistence window when the solvent is strongly selective. This is in agreement with previous experimental observations.<sup>12,13</sup> The



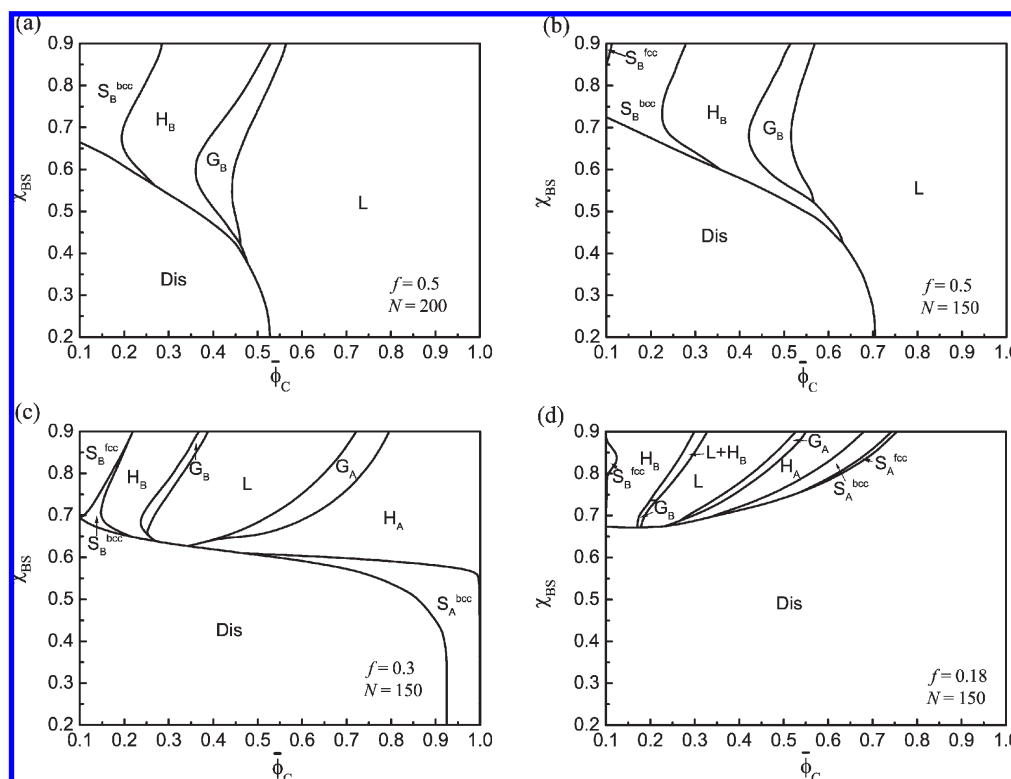


**Figure 1.** Two-dimensional phase diagram as a function of  $\bar{\phi}_C$  and  $\chi_{BS}$  for a diblock copolymer solution with  $\chi_{AB} = 0.1$ ,  $\chi_{AS} = 0.2$  and (a)  $f = 0.5$ ,  $N = 200$ ; (b)  $f = 0.5$ ,  $N = 150$ ; (c)  $f = 0.3$ ,  $N = 150$ ; (d)  $f = 0.18$ ,  $N = 150$ . The ordered phases are denoted as follows: L, lamellae; H, hexagonally packed cylinders; G, gyroid; S<sup>bcc</sup>, body-centered cubic spheres; S<sup>fcc</sup>, face-centered cubic spheres. Dis stands for the disordered phase. The subscript of each symbol refers to the core composition. The boundary between the regions of L + H<sub>B</sub> and G<sub>B</sub> should be considered just as a guide to the eye.

boundary between the regions of L + H and gyroid can be determined by the common tangent rule in principle, but it is hard to locate the boundary precisely by numerical methods. Thus the line we put there should be considered just as a guide to the eye.

As can be seen from Figure 1b–d, the existence window of the “inverted” fcc structure, S<sup>fcc</sup><sub>B</sub>, becomes larger than that of the “inverted” bcc structure, S<sup>bcc</sup><sub>B</sub>, when the copolymers become more asymmetric, i.e., the so-called “crew-cut” micelles (with small  $f$ ) favor the fcc structure, while “hairy” micelles (with larger  $f$ ) favor bcc structure. Also, at low temperature (large  $\chi_{BS}$ ) the system favors fcc structure, while at high temperature (small  $\chi_{BS}$ ), especially near the melting line, the system favors bcc structure. These behaviors are consistent with the experimental<sup>13,24</sup> and theoretical<sup>19,25,26</sup> results. Besides the reasons discussed in the above literatures, a possible mechanism may play the key role, which is the packing frustration.<sup>19,25</sup> Because of the incompressibility of the system, the spherical micelles must fill the whole space. Thus each micelle has to transmute its shape from sphere to that approaching the Wigner–Seitz cell of the ordered structure. This causes a conformational entropy reduction of each copolymer chain. This kind of transmutation is much harder for the “inverted” micelles than the normal micelles, because the outer part of each “inverted” micelle is composed of the shorter swollen blocks, which have less conformational entropy to adjust than that of the longer chains. Since the Wigner–Seitz cell of fcc lattice (dodecahedron) approaches a sphere more than that of bcc lattice (truncated octahedron), the “inverted” spherical micelles favor fcc packing when  $f$  becomes smaller, as shown from part b to part d in Figure 1.

To investigate the lyotropic transitions further, two ( $f, \bar{\phi}_C$ ) slices through the phase hypercube are given in Figure 2. As can be seen from Figure 2a, OOT lines all tilt to the right. This is a direct result of adding the solvent, which changes the effective composition of the diblock copolymer. (More discussions will be

given in next section.) While that  $\chi_{BS} = 0.65$  is just corresponding to the moderately selective solvent case, the addition of a strongly selective solvent always brings more complication to the system, which is indicated by Figure 2b. In this case of a strongly selective solvent, an obvious existence window of the “inverted” fcc spheres (i.e., S<sup>fcc</sup><sub>B</sub> in the range  $0.18 < f < 0.5$ ) is located as well as two normal close-packing structures. When  $f$  becomes small enough, neither G<sub>A</sub> nor G<sub>B</sub> is stable, and the L + H coexistence enters. On the other hand, lyotropic “reentrant” transitions can be observed when  $f$  is beyond 0.7. Because the solvent is A-selective in Figure 2, macrophase separation to a copolymer-rich phase and a solvent-rich phase must anticipate in the limit  $f \rightarrow 0$ . However, we do not find such a macrophase separation, at least in the parameter regions shown in Figure 2.

Figure 3 is of three ( $f, \chi_{BS}$ ) slices. The main progression in behavior follows from the previous perspective. For  $\bar{\phi}_C = 0.75$  (Figure 3a), the phase behavior of the system is only slightly different from the melt, and the diagram is approximately symmetric with respect to the axis of  $f = 0.5$ . For  $\bar{\phi}_C = 0.5$  (Figure 3b), the solvent selectivity has more apparent effects on the self-assembly of the copolymer. The regions of the structures on the right-hand side of L become broader while others are compressed. “Reentrant” OOTs accompanying with varying  $\chi_{BS}$  emerge in some regions of Figure 3 (b). For  $\bar{\phi}_C = 0.25$  (Figure 3, parts c and d), the A block of each copolymer is swollen much more than the B block. Thus the phases that are marked with a subscript A are stable only in a very small corner. Two L + H coexistence windows are also clear in this case.

## Discussions

In this section, we begin with some comments on the general features of phase behaviors of diblock copolymer solutions. Then two interesting phenomena, i.e., the L + H coexistence and the

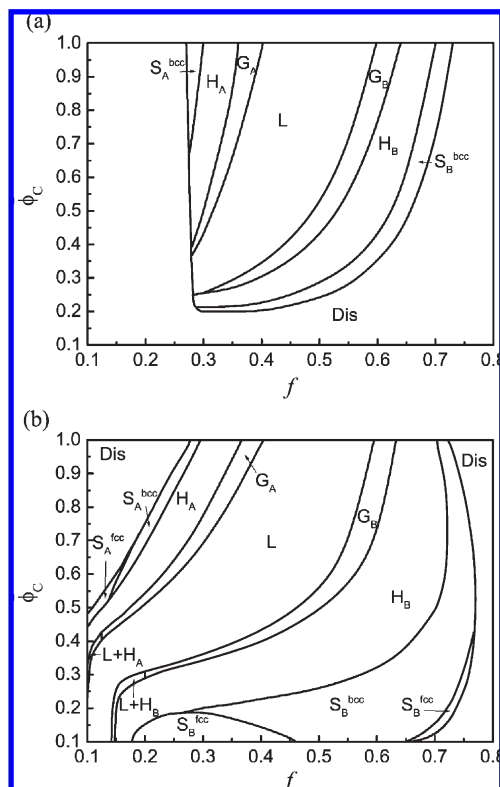


**Figure 2.** Two-dimensional phase diagram as a function of  $f$  and  $\bar{\phi}_C$  for a diblock copolymer solution with  $\chi_{AB} = 0.1$ ,  $\chi_{AS} = 0.2$ ,  $N = 150$  and (a)  $\chi_{BS} = 0.65$ ; (b)  $\chi_{BS} = 0.85$ . The meanings of the symbols are the same as Figure 1. The boundary between the regions of L + H and gyroid should be considered just as a guide to the eye.

transition between the “inverted” fcc structure and the “inverted” bcc structure, are discussed separately.

**General Comments.** Generally speaking, most of the phase transitions of a diblock copolymer solution can be comprehended by a simple intuitive geometric consideration, which is based on the relevant concepts of diblock copolymer melts<sup>19</sup> and summarized by Hanley and co-workers as “trajectory approach”.<sup>12</sup> The key point is that the addition of a selective solvent always makes the two blocks of the diblock copolymer unequally swollen, leading to changes of the effective composition of the copolymer and the degree of segregation of the system. Thus a sequence of transitions in a copolymer solution is generally corresponding to a tilting trajectory on the phase diagram of a neat copolymer. Take an AB-copolymer of  $f = 0.3$  as an example. In the melt state, it will display hexagonally packed cylinders,  $H_A$ . With the addition of an A-selective solvent, A-domains must be swollen more than B-domains, which corresponds to an increase of the effective composition. Therefore a sequence of  $H_A \rightarrow G_A \rightarrow L \rightarrow G_B \rightarrow H_B \rightarrow S_B^{bcc}$  via dilution can be expected if  $\chi_{BS}$  is large enough, which is verified in Figure 1c. The “reentrant” transitions in Figure 1 and Figure 3, which are obtained by changing  $\chi_{BS}$ , can be understood by a similar consideration. According to the discussions above, there are two factors to determine the structure of a copolymeric system. One is the degree of segregation, which corresponds to a vertical trajectory on the phase diagram of the melt case. The other is the effective composition of the copolymer, which corresponds to a horizontal trajectory. Changing  $\chi_{BS}$  will change these two factors simultaneously. However, when  $\bar{\phi}_C$  is low but  $\chi_{BS}$  is high (e.g., the area of  $\bar{\phi}_C < 0.5$  and  $\chi_{BS} > 0.75$  in Figure 1b), the system is in the strong segregation region where the stable structure of the system is

insensitive to the degree of segregation. For this case, the effective composition becomes the dominant factor. Then via decreasing  $\chi_{BS}$ , the degree of segregation lower, and it is necessary to consider both of the two factors to determine the equilibrium phase when  $\chi_{BS}$  is low enough (e.g.,  $\chi_{BS} < 0.7$  in Figure 1b). The system can have the same structure in the two limits and so a “reentrant” transition comes. The lyotropic ODT and OOT in Figure 2b can be discussed in a similar way except that the changes of these two factors now result from the dilution effect caused by the solvent.

It should be pointed out that when  $f < 0.1$  or  $\bar{\phi}_C < 0.1$ , the periodicity of each ordered phase becomes divergent quickly and the volume fraction of the solvent in the center of the major domain converges to a hundred percent due to our calculations (not shown here). This implies an existence of a disordered micelle state which cannot be verified rigorously in this work. Thus we only present the results in the area of  $f \geq 0.1$  and  $\bar{\phi}_C < 0.1$ .

**The L + H Coexistence.** Although the emergence of coexistence is not captured in previous discussions, it is not surprising in itself. Because all the OOTs examined here are of first order, coexistence region must be along each phase boundary when  $\bar{\phi}_C$  is set to be a variable. However, for most of the OOTs the coexistence window is very small. The typical value of the width,  $\Delta\bar{\phi}_C$ , of the coexistence window between adjacent structures is of order  $10^{-3}$ , which is much smaller than the resolution of any figure presented here. Contrarily, when the solvent is strongly selective and the copolymer is of high asymmetry in composition, the presumable location of gyroid phase between L and H is replaced by an L + H coexistence window, the width of which is of order 0.05 in terms of  $\Delta\bar{\phi}_C$ . Nevertheless, it should be noted that the L + H coexistence is peculiar in a sense, because L and H are not adjacent structures in the phase diagram of diblock copolymer melts. This is the reason why the L + H coexistence window can be much wider than the ones between adjacent structures.

It is well-known that the equilibrium structure of a conformationally symmetric diblock copolymer melt is attributed to the subtle balance of spontaneous curvature and packing frustration.<sup>19</sup> By this consideration, gyroid must exist as a consequence of a compromise between L and H in the case of copolymer melt. However, there can be another kind of compromise, i.e., the coexistence, in a solution. Then the phase behavior of the system is the result of the competition between these two possibilities. It is verified by the calculations that the existence window of gyroid becomes narrower with lowering  $f$  and increasing  $\chi_{BS}$ , which reflects a tendency of lifting of the corresponding free energy curve. Thus a replacement by L + H coexistence should occur when the free energy curve of gyroid is higher than the common tangent between L and H, which are adjacent to the gyroid. This kind of processes is illustrated in Figure 4. Figure 4 is the curves of reduced free energy,<sup>27</sup>  $F_{red}$ , for different phases around the boundary between the regions of L +  $H_B$  and  $G_B$  in Figure 1d. The lifting of the free energy curve of gyroid with respect to other curves accompanying with increasing  $\chi_{BS}$  is clear in this figure.

By similar considerations, other kinds of coexistence are also possible. However, they do not appear on the diagrams presented here from the calculations. Moreover, there is no experimental evidence for other kinds of coexistence either.

**The Transition between “Inverted” fcc and “Inverted” bcc.** There are two kinds of fcc-bcc transition in our system. One is the transition between the normal fcc and the normal bcc. This case has been discussed in detail elsewhere<sup>16,25</sup> and we do not intend to focus on this topic here. But it should be

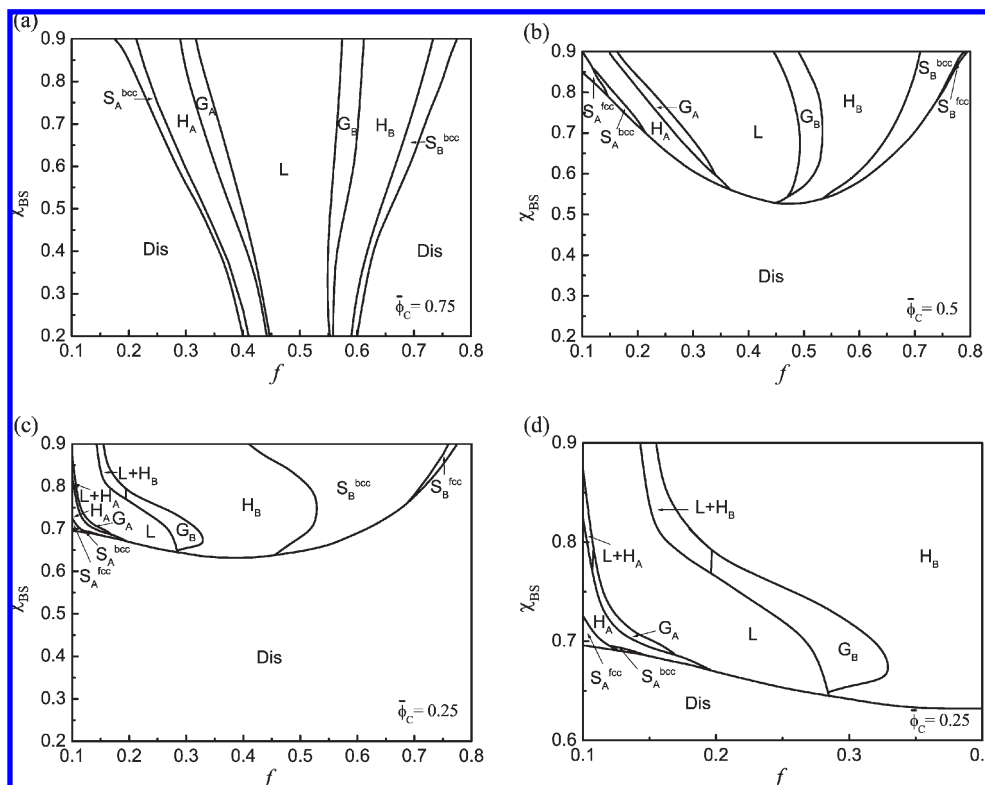


**Figure 3.** Two-dimensional phase diagram as a function of  $f$  and  $\chi_{BS}$  for a diblock copolymer solution with  $\chi_{AB} = 0.1$ ,  $\chi_{AS} = 0.2$ ,  $N = 150$  and (a)  $\bar{\phi}_C = 0.75$ , (b)  $\bar{\phi}_C = 0.5$ , (c)  $\bar{\phi}_C = 0.25$ , and (d)  $\bar{\phi}_C = 0.25$ . Figure 3d is the enlarged region in Figure 3c with  $0.1 \leq f \leq 0.4$  and  $0.6 \leq \chi_{BS} \leq 0.9$ . The meanings of the symbols are the same as Figure 1. The boundary between the regions of L + H and gyroid should be considered just as a guide to the eye.

pointed out that the normal fcc–bcc transitions usually occur near the ODT lines and thus are always concealed by fluctuation effects in practice.

The other kind of fcc–bcc transition is between “inverted” cubic phases, as can be seen in Figure 1b and Figure 2b. This is one of the most interesting phenomena in block copolymer solutions and much work has been done both experimentally and theoretically in order to explore the mechanism behind.<sup>24,26,28,29</sup> Our observation that “inverted” fcc packing is stable at low  $\bar{\phi}_C$  and large  $\chi_{BS}$  is qualitatively in agreement with previous studies. However, the mechanism of this kind of transition is still not very clear. The discussions on this topic before have always focused on the interaction between micelles, which cannot be verified directly by SCMFT calculations. Nevertheless, some hints can be obtained here. We decompose the free energy per monomer (eq 2) into three parts:

$$\frac{F_{CS}}{\rho_0 V k_B T} = \frac{1}{V} \int d\mathbf{r} [\chi_{AS} \phi_A(\mathbf{r}) \phi_S(\mathbf{r}) + \chi_{BS} \phi_B(\mathbf{r}) \phi_S(\mathbf{r})] \quad (10)$$

$$\begin{aligned} \frac{F_{AB}}{\rho_0 V k_B T} = & \frac{1}{V} \int d\mathbf{r} [\chi_{AB} \phi_A(\mathbf{r}) \phi_B(\mathbf{r}) \\ & - \frac{1}{N} \omega_A(\mathbf{r}) \phi_A(\mathbf{r}) - \frac{1}{N} \omega_B(\mathbf{r}) \phi_B(\mathbf{r})] - \frac{\bar{\phi}_C}{N} \ln Q_C \end{aligned} \quad (11)$$

$$\frac{F_S}{\rho_0 V k_B T} = -\frac{1}{NV} \int d\mathbf{r} \omega_S(\mathbf{r}) \phi_S(\mathbf{r}) - \bar{\phi}_S \ln Q_S \quad (12)$$

where the unimportant constants are ignored. Obviously,  $F_{CS}$  is the contribution of the interaction between solvents

and AB-copolymers;  $F_S$  is the contribution of the translational entropy of the solvents;  $F_{AB}$  is the contribution to the free energy by AB-copolymers themselves. Then the difference between the free energies of “inverted” fcc and “inverted” bcc,  $\Delta F_{\text{tot}}$ , is also composed of three parts:

$$\Delta F_{\text{tot}} = \Delta F_{CS} + \Delta F_{AB} + \Delta F_S$$

where

$$\Delta F_{\alpha} = \frac{F_{\alpha}^{\text{fcc}} - F_{\alpha}^{\text{bcc}}}{\rho_0 V k_B T}$$

with  $\alpha = \text{CS, AB, and S}$ .

Figure 5 shows the free energy difference per monomer (in the unit of  $10^{-5} k_B T$ ) between “inverted” fcc and “inverted” bcc as a function of  $\chi_{BS}$ . Figure 5a is for the case of  $f = 0.3$  and  $\bar{\phi}_C = 0.15$ . In this case, the structure of the system is “inverted” fcc for high  $\chi_{BS}$  and transforms into “inverted” bcc when  $\chi_{BS} \approx 0.76$  as indicated by the dash-dot-dot line. As can be seen from Figure 5a,  $\Delta F_{AB}$  always has negative value and hence favors fcc packing. However, it is also indicated by the figure that  $\Delta F_{AB}$  is less important for most cases. The main contributions to  $\Delta F_{\text{tot}}$  are made by the terms of  $\Delta F_{CS}$  and  $\Delta F_S$ . Nevertheless,  $\Delta F_S$  is positive to the “right” of the transition line where  $\Delta F_{\text{tot}}$  is negative. This disfavor to the structure of “inverted” fcc is conquered by the  $\Delta F_{CS}$  term. Figure 5b is for the case of a symmetric diblock copolymer solution at the same concentration as Figure 5a.<sup>30</sup> In this case, the signs of  $\Delta F_{CS}$  and  $\Delta F_S$  are opposite to those in Figure 5a. But  $S_B^{\text{bcc}}$  is the stable structure now and so the equilibrium structure is also stabilized by the  $\Delta F_{CS}$  term. In a word, it is indicated by Figure 5 that the solvent–copolymer

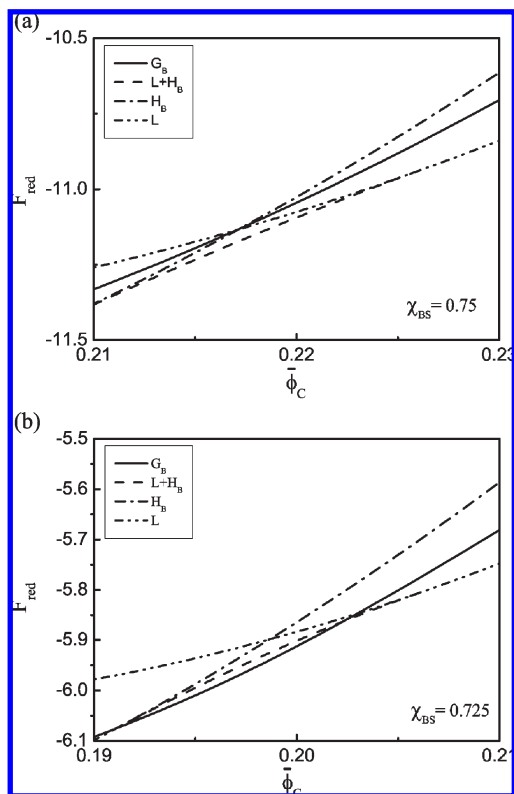


**Figure 4.** The reduced free energy (in units of  $10^{-4}k_B T$ ) of different phases as functions of  $\phi_C$  with  $\chi_{AB} = 0.1$ ,  $\chi_{AS} = 0.2$ ,  $N = 150$ ,  $f = 0.18$ : (a)  $\chi_{BS} = 0.75$ ; (b)  $\chi_{BS} = 0.725$ .

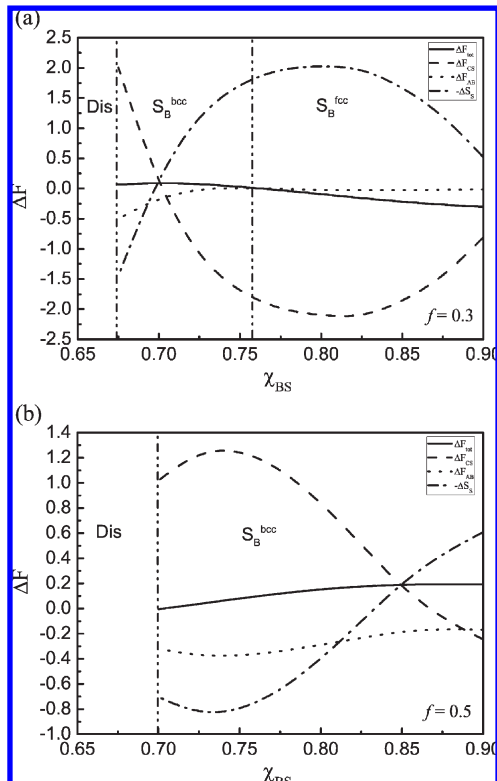


**Figure 5.** Free energy difference per monomer (in the unit of  $10^{-5}k_B T$ ) between “inverted” fcc and “inverted” bcc as a function of  $\chi_{BS}$  with  $\chi_{AB} = 0.1$ ,  $\chi_{AS} = 0.2$ ,  $N = 150$ , and  $\phi_C = 0.15$ : (a)  $f = 0.3$ ; (b)  $f = 0.5$ . The dash-dot-dot lines indicate the phase transition points between different structures.

interaction plays an important role in the “inverted” fcc–bcc transition.

## Conclusions

We have employed an SCMFT calculation to investigate the phase behaviors of AB-diblock copolymer solutions. Several slices through the phase hypercube have been presented in order to give a comprehensive description. As can be seen from the phase diagrams, the system of high  $\phi_C$  has similar behaviors of the melt case. Upon dilution, series of phase transitions occur. While a strongly selective solvent makes the self-assembling behavior diverse, the case of a weakly selective solvent is as simple as the neutral solvent case. Most transitions on the phase diagrams can be regarded as direct results of the nonuniformly distributing of the solvent into the domains of the two species.

In addition to the general transitions, some interesting features do come. First, wide windows of lamellae + cylinder coexistence are located for the cases of highly asymmetric diblock copolymers in strongly selective solvents, which is in agreement with previous experimental observations. Second, the transitions between “inverted” fcc and “inverted” bcc have been observed. It is indicated by our calculation that the solvent-copolymer interaction is a key point to understand the transitions of this kind, although the mechanism underneath still needs further exploration.

**Acknowledgment.** We acknowledge the helpful discussions with Shuanhu Qi, Xinghua Zhang, and Xingkun Man. This work is supported by the National Natural Science Foundation of China (NSFC), Grants 20874111 and 50821062, and by the Chinese Academy of Sciences, Grant KJCX2-YW-206.

**Note Added after ASAP Publication.** This article posted ASAP on July 31, 2009. In the section “More about the Model”, a typographical change has been made in the equation describing the estimate of selectivity. The correct version posted on August 5, 2009.

## References and Notes

- Helfand, E.; Tagami, Y. *J. Chem. Phys.* **1972**, *56*, 3592.
- Hong, K. M.; Noolandi, J. *Macromolecules* **1983**, *16*, 1083.
- Fredrickson, G. H.; Leibler, L. *Macromolecules* **1989**, *22*, 1238.
- Olvera de la Cruz, M. *J. Chem. Phys.* **1989**, *90*, 1995.
- Whitmore, M. D.; Noolandi, J. *J. Chem. Phys.* **1990**, *93*, 2946.
- Whitmore, M. D.; Vavasour, J. D. *Macromolecules* **1992**, *25*, 2041.
- Lodge, T. P.; Hanley, K. J.; Pudil, B.; Alahapperuma, V. *Macromolecules* **2003**, *36*, 816.
- Shibayama, M.; Hashimoto, T.; Kawai, H. *Macromolecules* **1983**, *16*, 16.
- Hashimoto, T.; Shibayama, M.; Kawai, H.; Watanabe, H.; Kotaka, T. *Macromolecules* **1983**, *16*, 361.
- Hajduk, D. A.; Kossuth, M. B.; Hillmyer, M. A.; Bates, F. S. *J. Phys. Chem. B* **1998**, *102*, 4269.
- Hanley, K. J.; Lodge, T. P. *J. Polym. Sci., Part B: Polym. Phys.* **1998**, *36*, 3101.
- Hanley, K. J.; Lodge, T. P.; Huang, C. I. *Macromolecules* **2000**, *33*, 5918.
- Lodge, T. P.; Pudil, B.; Hanley, K. J. *Macromolecules* **2002**, *35*, 4707.
- Banaszak, M.; Whitmore, M. D. *Macromolecules* **1992**, *25*, 3406.
- Huang, C. I.; Lodge, T. P. *Macromolecules* **1998**, *31*, 3556.
- Huang, C. I.; Hsueh, H. Y. *Polymer* **2006**, *47*, 6843.
- Woloszczuk, S.; Banaszak, M.; Knychala, P.; Radosz, M. *Macromolecules* **2008**, *41*, 5945.
- Lennon, E. M.; Katsov, K.; Fredrickson, G. H. *Phys. Rev. Lett.* **2008**, *101*, 138302.
- Matsen, M. W. *J. Phys.: Condens. Matter* **2002**, *14*, R21.
- Shi, A. C. Self-Consistent Field Theory of Block Copolymers. In *Developments in Block Copolymer Science and Technology*; Hamley, I. W., Ed.; John Wiley and Sons, Ltd.: New York, 2004; Chapter 8.

- (21) Henry, N. F. M.; Lonsdale, K. *International Tables for X-ray Crystallography*; Kynoch: Birmingham, U.K., 1969.
- (22) Vavasour, J. D.; Whitmore, M. D. *Macromolecules* **2001**, *34*, 3471.
- (23) Cochran, E. W.; Garcia-Cervera, C. J.; Fredrickson, G. H. *Macromolecules* **2006**, *39*, 2449.
- (24) McConnell, G. A.; Gast, A. P.; Huang, J. S.; Smith, S. D. *Phys. Rev. Lett.* **1993**, *71*, 2102.
- (25) Matsen, M. W. *Macromolecules* **1995**, *28*, 5765.
- (26) Grason, G. M. *J. Chem. Phys.* **2007**, *126*, 114904.
- (27) The reduced free energy in Figure 4 is the free energy difference between each ordered structure and the disordered phase, for the purpose of making the figure clearer. The unimportant free energy curves of fcc and bcc are omitted.
- (28) Bang, J.; Lodge, T. P.; Wang, X.; Brinker, K. L.; Burghardt, W. R. *Phys. Rev. Lett.* **2002**, *89*, 215505.
- (29) Lodge, T. P.; Bang, J.; Park, M. J.; Char, K. *Phys. Rev. Lett.* **2004**, *92*, 145501.
- (30) Note that  $f = 0.5$  is a critical composition, beyond which no "inverted" structure can form in this work.